A Self-Tuning Regulator for the High-Precision Position Control of a Linear Switched Reluctance Motor

Shi Wei Zhao, *Student Member, IEEE*, Norbert C. Cheung, *Senior Member, IEEE*, Wai-Chuen Gan, *Senior Member, IEEE*, Jin Ming Yang, and Jian Fei Pan, *Student Member, IEEE*

***Abstract*—In the high-technology mass manufacturing industry, high-speed and high-precision motion is an indispensable element in the automated production machines. In recent years, there has been a growing tendency to employ direct drive permanent magnet linear synchronous motors in demanding motion applications. Although the overall performance is good, its implementation cost remains high. This is mostly due to the cost of the Neodymium–Boron magnets, the manufacturing of the magnetic rails, and the precision of the overall mechanics. In this paper, a much cheaper alternative is proposed-to use a low-cost linear switched reluctance motor (LSRM) and an adaptive control strategy to overcome the tolerances and difficult control characteristics inherent in the motor. The LSRM has simple and robust structure, and it does not contain any magnets. However, its force is solely drawn from the reluctance change between the coil and the steel plates. Variations on the behavior of these two elements due to different operating conditions will change the motion behavior of the motor. Also, to keep the overall cost low, the LSRM sets a marginal mechanical tolerance during its mass production. This leads to characteristic variations in the final product. Finally, since the LSRM is a direct drive motor, any variations on the motor characteristics will directly reflect on the control system and the motion output. In this paper, a self-tuning regulator (STR) is proposed to combat the difficulties and uncertain control behaviors of the LSRM. This paper first introduces the motor winding excitation scheme, the model of the LSRM, and the current control method. The LSRM system is modeled as a single-input single-output discrete model with its parameters estimated by the recursive least square (RLS) algorithm. Then, an STR based on the pole placement algorithm is applied to the LSRM for high-performance position tracking. Both the simulation investigation and the experimental verification were conducted. In both cases, the results verified that the proposed RLS algorithm can estimate the parameters with fast convergence. The STR can provide quick response and high precision which is robust to the change of system parameters. Combined with STR control, the LSRM is a low-cost solution to fast, accurate, and reliable position tracking for many demanding motion control applications.**

Manuscript received March 30, 2006; revised August 28, 2006. This work was supported in part by the Hong Kong Polytechnic University under Project BQ831, by the University Grants Council under Project PolyU 5224/04E, and by the South China University of Technology through the National Science Foundation of China (60674099).

S. W. Zhao, N. C. Cheung, and J. F. Pan are with the Department of Electrical Engineering, Hong Kong Polytechnic University, Hunghom, Kowloon, Hong Kong (e-mail: eencheun@polyu.edu.hk).

W.-C. Gan is with the Motion Group, ASM Assembly Automation Hong Kong, Ltd., Kwai Chung, NT, Hong Kong (e-mail: wcgan@asmpt.com).

J. M. Yang is with the Electric Power College, South China University of Technology, Guangzhou 510640, China (e-mail: jmyang@scut.edu.cn).

Digital Object Identifier 10.1109/TIE.2007.900348

***Index Terms*—Linear switched reluctance motor (LSRM), motor winding excitation scheme, position control, self-tuning regulator (STR).**

I. Introduction

THE linear switched reluctance motor (LSRM) has a simple structure; it is rugged, reliable and low in cost. It is also capable of operating in harsh environments and wide speed range. Therefore, LSRM is an attractive candidate for position or velocity control. LSRM has certain advantages when it is used as a high-speed and high-precision linear motion system. Compared with rotary motor coupled with rotary-to-linear mechanical translator, LSRM has a quicker response, high-sensitivity, and high-tracking capability. Compared to direct drive permanent magnet linear synchronous motor, LSRM has a simpler and rugged structure, and a lower system cost. On the downside, LSRM is difficult to control and its output has a higher force ripple. This is due to the complex and nonlinearity of the LSRM magnetic circuit, which is difficult to model, simulate, and control.

In recent years, LSRM for high-performance motion control has attracted renewed interest, and there have been several reports on the different aspects of the LSRM. The design schemes and analysis for LSRM are presented in [2]–[6]. References [3] and [4] discuss the design aspects of the LSRM for precision position control applications. Speed control for LSRM is discussed in [7]–[9]. A current controller and a speed controller are proposed in [7], and an autodisturbance rejection controller is applied to the speed control for LSRM in [9]. The initial problems of precision position control in LSRM are tackled in [12]. The authors propose a simple position controller based on a nonlinear compensation table to linearize the relationships between force, current, and position in the LSRM. However, this method is based on a direct lookup table; it does not take into account of load variation and parameter change. This method is improved in [10] by adding a plug-in compensator to allow for small variations in the nonlinear compensation table. So far, in the publications of high-precision position control of LSRM, there has been no mention of an adaptive controller which observes and regulates the whole model of the LSRM, including its electrical, magnetic, and mechanical behaviors.

The control of LSRMs requires proper synchronization with current position. Moreover, the electromagnetic force with

ripples is nonlinear with different positions and current levels. The force ripples degrade tracking ability of the LSRMs remarkably. Manufacturing imperfection, such as the variation of the air gap, can result in characteristic differences during the mass production. Moreover, the parameters of the LSRM system often change with operating conditions and time. For example, the motor winding resistance changes with temperature and the frictional force of the linear motion guide changes with time. These would eventually contribute to the motor model uncertainties. For high-performance LSRM drives, online parameter identification is a useful method, since static models are hard to represent the real machine adequately during dynamic operating conditions. Moreover, self-tuning regulators (STRs) can avoid adjusting controller parameters for different LSRMs applications. There are few literatures applying STR to position tracking of LSRMs. This paper intends to develop a STR with online parameter identification which considers winding current tracking and the LSRM together as a controlled plant. Here, the controlled plant is regarded as a second-order system since the control bandwidth of the current tracking is much quicker than that of the position tracking loop in this system. The STR adopts pole placement method to update the control parameters. Also, the parameters of the total controlled plant are estimated by the recursive least square (RLS) algorithm, which can get more accurate estimation and robust to the measurement noise.

The organization of this paper is as follows. Construction and modeling of the LSRM are given in Section II and parameter identification and STR design in Section III. Sections IV–VI present the simulation results, experimental results, and conclusions, respectively.

II. Construction and Modeling of LSRM

A. Configuration of LSRM

The design schematic of the LSRM system is showed in Fig. 1. A set of three-phase coils are installed on the moving platform as shown in Fig. 1. The three coils are with same dimension. The body of the moving platform is manufactured with aluminum, so that the total weight of the moving platform and its inertia are low and the magnetic paths are decoupled. The moving platform is mounted on two slider blocks, which are tightly fixed on the bottom of the LSRM. Also, between the moving platform and the slider blocks, there are some ball bearings. This rugged mechanical structure can effectively buffer vibration in operation. The stator track and the core of the windings are laminated with 0.5-mm silicon–steel plates. A 0.5-μm-resolution linear optical encoder is integrated in the LSRM system to observe the motion profile of the moving platform and provide the feedback position information. The electrical and mechanical parameters of the LSRM are listed in Table I.

B. Modeling of LSRM

The LSRM system has a highly nonlinear characteristic due to its nonlinear flux behavior. The fundamental equations of LSRMs are the voltage balancing (1), the electromagnetic force production (2), and the mechanical movement (3). Here, ν_j is the voltage applied to the terminals of phase j, i_j is the current of phase j, r_j is the winding resistance, λ_j is the phase flux linkage of phase j, x is the displacement, $f_{\rm e}$ is the generated electromagnetic force, $f_{\rm l}$ is the external load force, and M and B are the mass and friction constant, respectively,

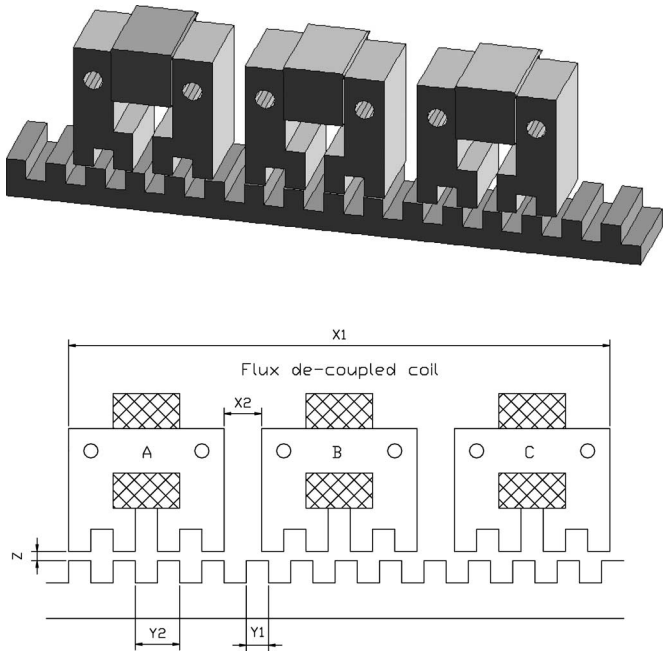

Fig. 1. Schematic of the LSRM.

$$\nu_j = r_j i_j + \frac{d\lambda_j}{dt}, \qquad j = a, b, c \tag{1}$$

$$f_{\rm e} = \sum_{j=a}^{c} \frac{\partial \int_0^{i_j} \lambda_j di_j}{\partial x} \tag{2}$$

$$f_{\rm e} = M\frac{d^2x}{dt^2} + B\frac{dx}{dt} + f_{\rm l}. \tag{3}$$

In general, the mechanical time constant is much slower than the electrical time constant of the current tracking loop. The above claim is justified for our test setup since we can achieve the current loop bandwidth up to kilohertz while the output mechanical bandwidth is on the order of 10 Hz [10]. Therefore, the two-time-scale analysis and design can be applied in the LSRM system. The dynamics of the mechanical position is slower than that of the electrical current. When the mechanical variables are mainly discussed, the electromagnetic variables can be regard as constants. As a result, the electromagnetic force production equation can be approximated as

$$f_j(x, i_j) = \frac{1}{2}\frac{dL_j}{dx} i_j^2, \qquad j = a, b, c \tag{4}$$

where f_j is the generated electromagnetic force of phase j, dL_j/dx is the inductance change rate of phase j. One characteristic of LSRMs is that it must be driven synchronously with its position. Generally, the motor winding excitation scheme for LSRMs can be considered as a force distribution function (FDF) and an approximated function of inductance change rate and the scheme of the driver can be shown in Fig. 2. The

TABLE I
ELECTRICAL AND MECHANICAL PARAMETERS OF THE LSRM

Pole width (y_1)	6mm
Pole pitch (y_2)	12mm
Motor length (x_1)	146mm
Phase separation (x_2)	10mm
Winding length	30mm
Wind width	25mm
Air gap width (z)	0.5mm
Phase resistance	2.5Ω
Aligned inductance	19.2mH
Unaligned inductance	11.5mH
Mass of the moving platform (M)	1.8Kg
Friction constant (B)	0.08N*s*m^{-1}

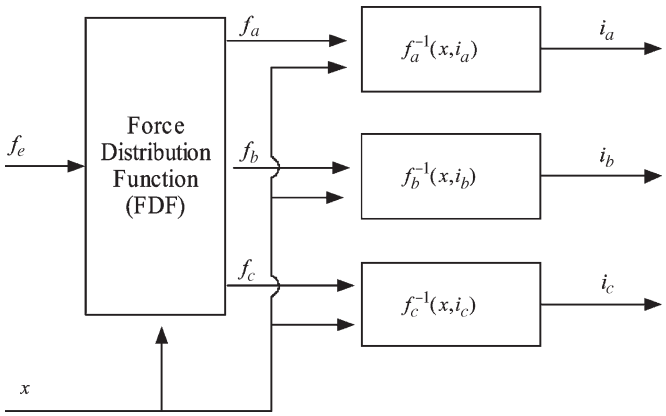

Fig. 2. Scheme of the LSRM driver.

FDF is used to compute the force for each phase according to the position and the direction. The approximated function of inductance change rate is used to compute the phase current according to the command force of phase and the position. Some methods have been proposed for the approximated function of inductance change rate [7]–[11]. They can be classified into two types: the type of lookup table and the type of approximated function. If the FDF and the approximated function of inductance change rate are chosen, the current can be calculated by the inverse function $f_j^{-1}(x, i_j)$ of (4) with command force and its position. In this paper, the FDF is chosen as in Table II [10] and the approximated function of inductance change rate is described as [11]

$$\frac{dL_j\left(x_j(t)\right)}{dx_j(t)} = -K_{pj}\sin\left(\frac{2\pi x_j(t)}{y_2}\right), \qquad j = a, b, c$$
$$x_b = x_a + \frac{2y_2}{3}$$
$$x_c = x_a + \frac{y_2}{3}. \tag{5}$$

Here, y_2, x_j, and K_{pj} are the pole pitch of the LSRM, the displacement of phase j and a proportional parameter, respectively.

According to the approximated function of inductance change rate in (5) and the FDF in Table II, the output force experiment is performed on the proposed LSRM. The experimental data is shown in Fig. 3. From the figure, the output force is found to increase with the command force and the change rate of output force is almost kept as a constant value to the same position. However, there are output force ripples at the same force command when the position changes. The output force is nonlinear to the position and force command. The parameters of the LSRM system change with its position and force command when it runs. Static models are hard to represent the real machine adequately during dynamic operating condition. Online parameter identification is a useful method for real-time parameter estimation, which can provide information to describe the parameter changes. In this paper, the parameters of the LSRM are online estimated by RLS algorithm. According to the two-time-scale analysis, the LSRM can be considered as a second-order system with the current tracking controller [7] when the dynamics of the currents are ignored. If $y(t)$ is defined as the output of a plant, $u(t)$ is defined as the input of the plant, $w(t)$ is defined as the load disturbance, and q is defined as the forward shift operator, the second-order system can be rewritten as the single-input single-output discrete model given by

$$A(q)y(t) = B(q)\left[u(t) + w(t)\right] \tag{6}$$

where

$$A(q) = q^2 + a_1 q + a_2 \quad \text{and} \quad B(q) = b_0 q + b_1.$$

III. STR DESIGN FOR THE LSRM

The STR can automatically tune its parameters to obtain the desired performances of the closed-loop system. Fig. 4 shows the fundamental construction of the STR. In each control cycle of the STR, there are three steps included. The first step is to identify the parameters of the plant; in the second step, the parameters of the controller are decided on the basis of the

TABLE II
FDF SCHEME

Position range	+ve force command	-ve force command
0mm-2mm	$f_B=f_x$	$f_C=0.5(2-x)f_x$, $f_A=0.5xf_x$
2mm-4mm	$f_B=0.5(4-x)f_x$, $f_C=0.5(x-2)f_x$	$f_A=f_x$
4mm-6mm	$f_C=f_x$	$f_A=0.5(6-x)f_x$, $f_B=0.5(x-4)f_x$
6mm-8mm	$f_C=0.5(8-x)f_x$, $f_A=0.5(x-6)f_x$	$f_B=f_x$
8mm-10mm	$f_A=f_x$	$f_B=0.5(10-x)f_x$, $f_C=0.5(x-8)f_x$
10mm-12mm	$f_A=0.5(12-x)f_x$, $f_B=0.5(x-10)f_x$	$f_C=f_x$

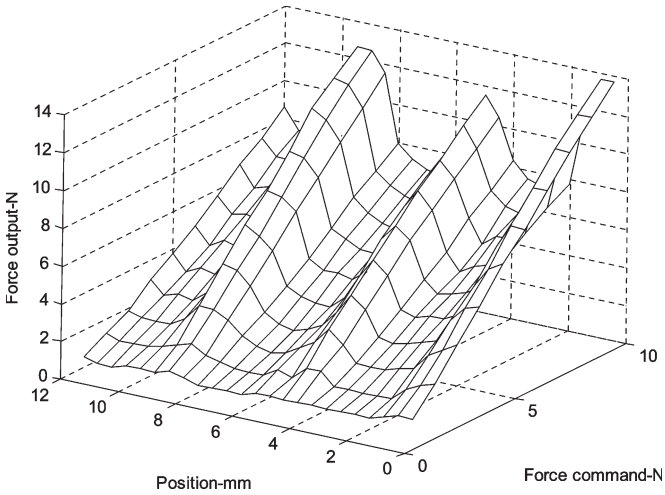

Fig. 3. Force command versus position versus force output 3-D chart.

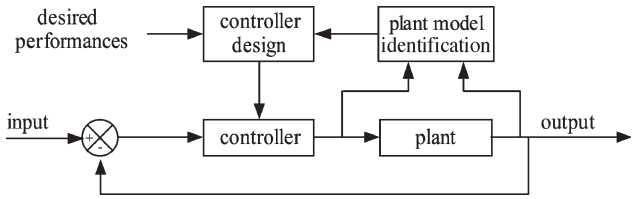

Fig. 4. Construction of the STR.

result of the identification and the desired performances; and the control signal is calculated using the parameters of the controller, input signal, and output signal.

A. Parameter Identification of LSRM

The design of a STR is based on the online parameter identification, which can represent the dynamics of the actual plant in real time. As discussed before, the LSRM is assumed as a second-order system as (6). It can be seen that the load disturbances contaminate the input signals and they can eventually result in the error of the estimation. Therefore, some filtering and pretreatment are required before the input and output signals are used for the parameter identification. Usually, the load disturbances cannot be measured and is used for the estimation directly. However, they can be considered as a relatively slow variable and can be diminished by a filter as follows [1], [13]:

$$\overline{u}(t) = \alpha\overline{u}(t-1) + u(t) - u(t-1)$$
$$\overline{y}(t) = \alpha\overline{y}(t-1) + y(t) - y(t-1), \qquad 0 \le \alpha \le 0.5$$

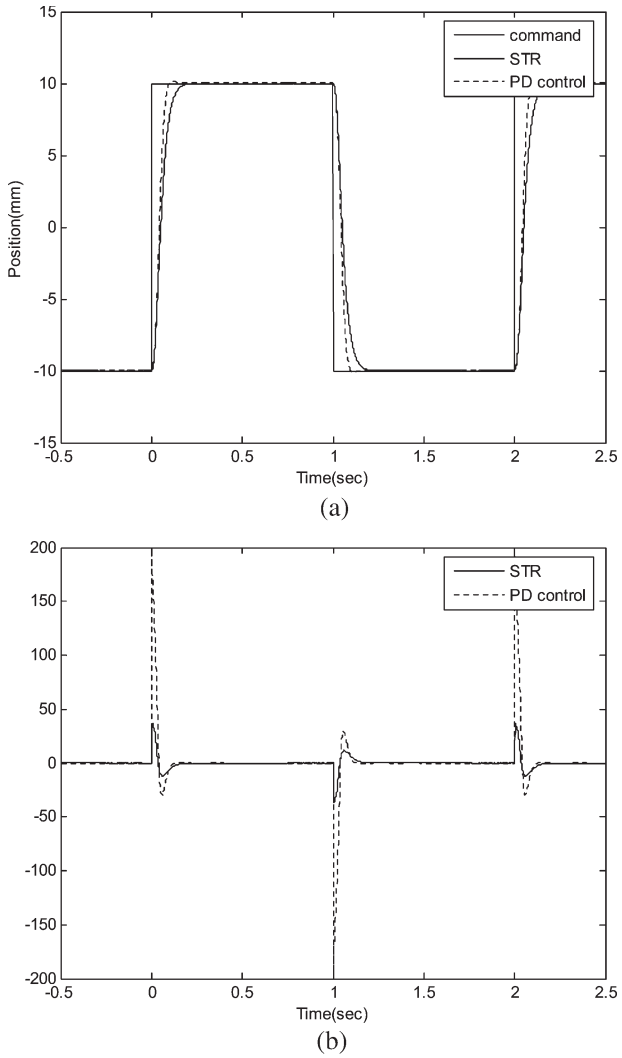

Fig. 5. (a) Trajectory response and (b) control signal of the LSRM system.

where $\overline{u}(t)$ and $\overline{y}(t)$ are the filtered input and output, respectively.

Therefore, the system model (6) can be rewritten as (7), which can be parameterized as (8)

$$A(q)\overline{y}(t) = B(q)\overline{u}(t) \tag{7}$$
$$\overline{y}(t) = \varphi^{\mathrm{T}}(t-1)\theta(t-1) + \varepsilon(t) \tag{8}$$

where $\theta = [a_1, a_2, b_0, b_1]$, $\varphi^{\mathrm{T}}(t-1) = [-\overline{y}(t-1), -\overline{y}(t-2), \overline{u}(t-1), \overline{u}(t-2)]$, and $\varepsilon(t)$ is the residuals.

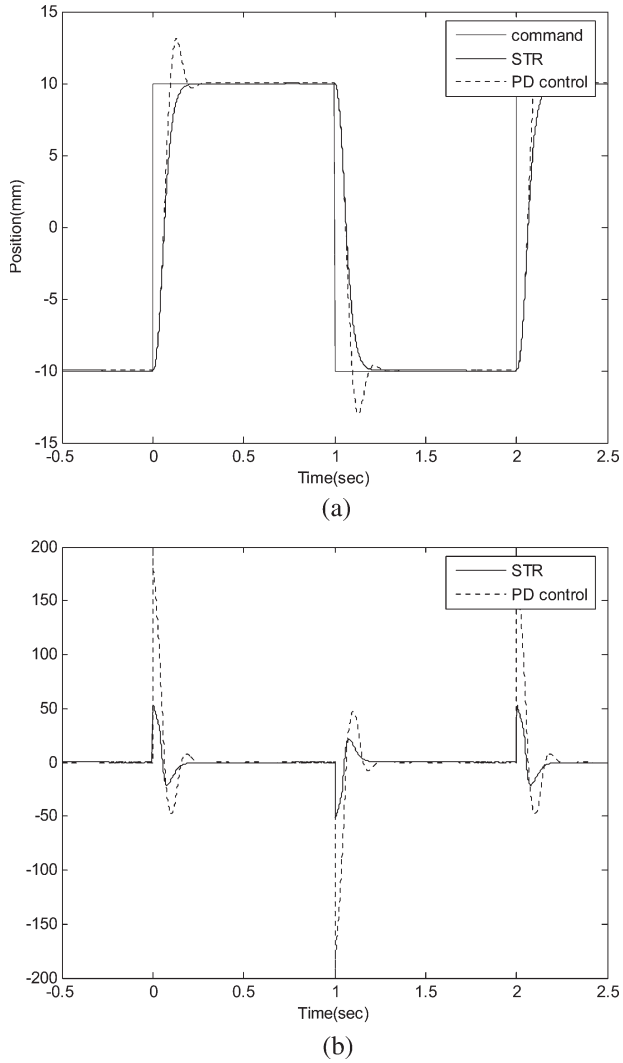

Fig. 6. (a) Trajectory response and (b) control signal of the LSRM system during its simulation with the 200% mass increase on the moving platform.

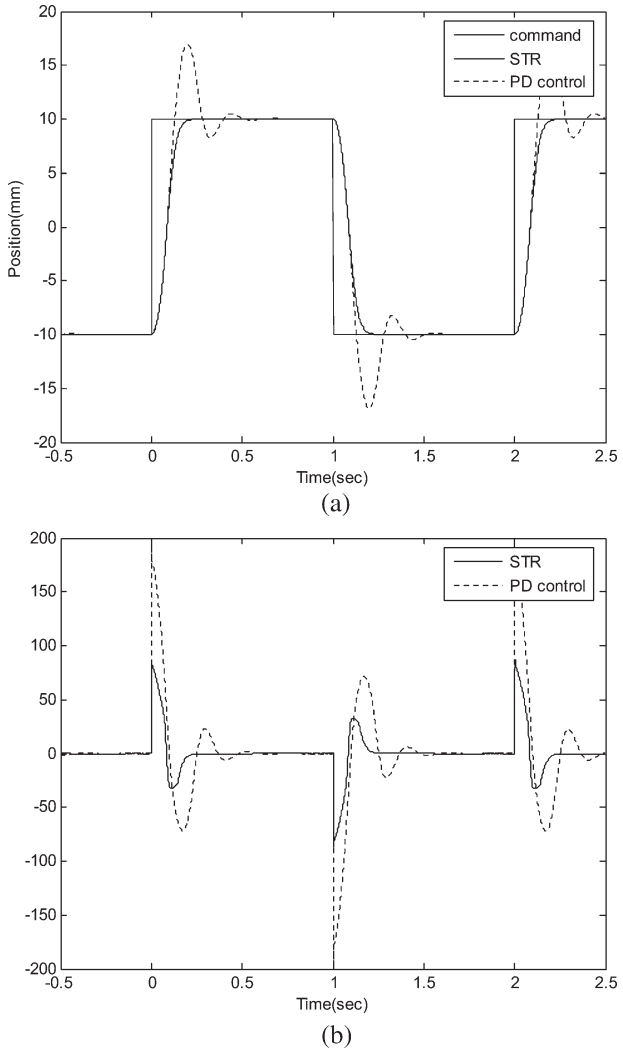

Fig. 7. (a) Trajectory response and (b) control signal of the LSRM system during its simulation with 50% system gain and 200% mass increase on the moving platform.

Parameters of (8) can be estimated by the RLS algorithm [1] as

$$\theta(t) = \theta(t-1) + K(t)\left[\overline{y}(t) - \varphi^{\mathrm{T}}(t)\theta(t-1)\right] \tag{9}$$

$$K(t) = P(t-1)\varphi(t)\left[\lambda + \varphi^{\mathrm{T}}(t)P(t-1)\varphi(t)\right]^{-1} \tag{10}$$

$$P(t) = \frac{1}{\lambda}[I - K(t)\varphi^{\mathrm{T}}(t)]P(t-1) \tag{11}$$

where P is the covariance matrix and λ is the forgetting factor. $K(t)$ can be interpreted as the adjusting gain. If $K(t) = 0$, the estimated parameters θ converge to some constants. The forgetting factor, λ, which can be given from 0 to 1, reflects the parameter converging rate. If the forgetting factor is set at a small value, the estimated parameters would converge quickly with big ripples. On the other hand, when the forgetting factor is given a big value, the estimated parameters would converge slowly with small ripples. Here, forgetting factor is given by 0.999. The initial covariance matrix $P(0)$ is selected as rI_4, which is a 4-D unit matrix I_4 scaled by a positive scalar r, here r is given as a value of 10. Also, for the RLS algorithm, persistent excitation is required to make the estimated parameters to converge to their real values.

B. STR Design for LSRM

In this paper, the STR is designed by the pole placement algorithm. For a plant described as (6), a general linear regulator can be described by

$$R(q)u(t) = T(q)u_{\mathrm{c}}(t) - S(q)y(t) \tag{12}$$

where $R(q)$, $S(q)$, and $T(q)$ are polynomials, $u_{\mathrm{c}}(t)$ is the command input signal. To obtain a causal regulator in the discrete time case, the following conditions must be imposed: $\deg S \leq \deg R$ and $\deg T \leq \deg R$. Also, the closed-loop equation can be obtained as (13) by combining (6) with (12). From (13), the

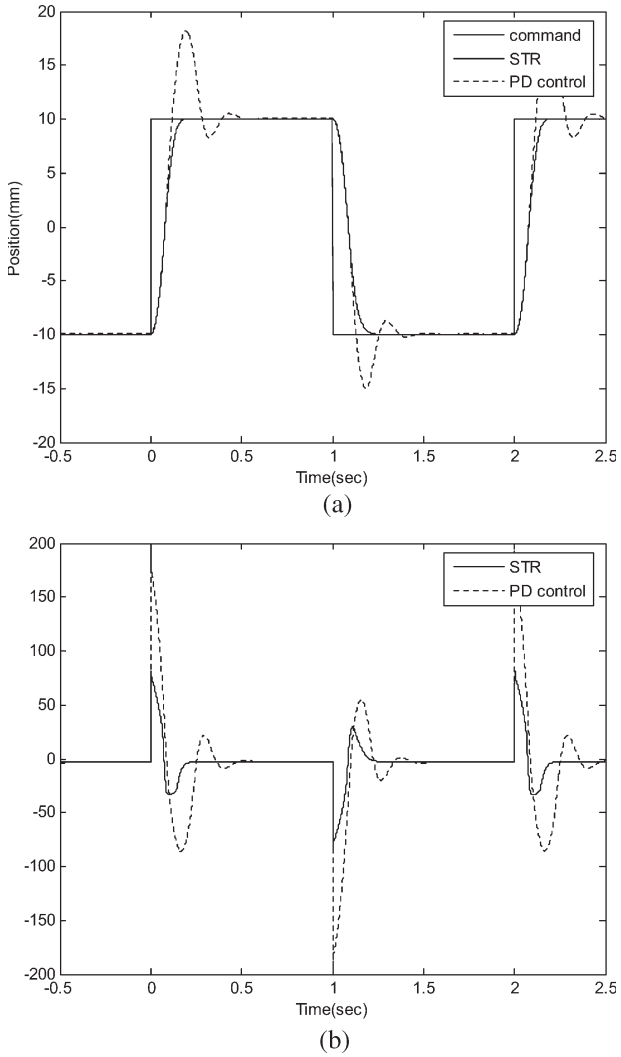

Fig. 8. (a) Trajectory response and (b) control signal of the LSRM system during its simulation with 50% system gain, 200% mass increase, and an external load disturbance on the moving platform.

system output is considered as the result acted by the command input signal and the external load disturbances

$$y(t) = \frac{B(q)T(q)}{A(q)R(q) + B(q)S(q)} u_{\mathrm{c}}(t) + \frac{B(q)R(q)}{A(q)R(q) + B(q)S(q)} w(t). \quad (13)$$

If the desired response from the command signal $u_{\mathrm{c}}(t)$ to the output $y_m(t)$ is set as the dynamics (14), the (15) should be satisfied for model following. $R^0(q)$, $S^0(q)$, and $T^0(q)$ are the solutions to the (15), $A_0(q)$ is the observer polynomial. The causality conditions for (15) can be accordingly written as

$$A_m(q)y_m(t) = B_m(q)u_{\mathrm{c}}(t) \quad (14)$$

$$\frac{B(q)T^0(q)}{A(q)R^0(q) + B(q)S^0(q)} = \frac{A_0(q)B_m(q)}{A_0(q)A_m(q)} \quad (15)$$

$$\deg A_0 + \deg A_m \geq 2\deg A - 1$$

$$\deg A_m - \deg B_m \geq \deg A - \deg B. \quad (16)$$

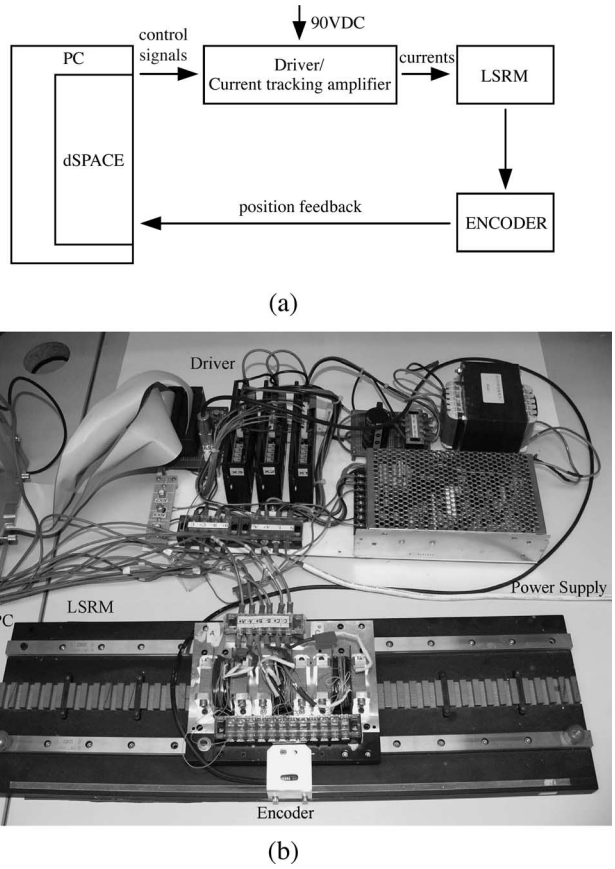

Fig. 9. Experimental setup of the LSRM motion system: (a) the block diagram and (b) the overall appearance.

In many cases, the loading disturbances are relatively slow to the command input signals. Here, the disturbance $w(t)$ is assumed to satisfy the following equation:

$$(q-1)w(t) = e(t) \quad (17)$$

where $e(t)$ is a white noise. The influence of the disturbance to the system output is represented by the second polynomial on the right-hand side of the (13). To cancel the influence of the disturbance, a factor as $q-1$ can be included in $R(q)$. This may be achieved by requiring that $R(q)$ have the form

$$R(q) = (q-1)R'(q)$$

where $R'(q)$ is a polynomial. Therefore, if $R(q)$, $S(q)$, and $T(q)$ satisfy the following:

$$\begin{aligned} R(q) &= (q-1)R'(q) = X(q)R^0(q) + Y(q)B(q) \\ S(q) &= X(q)S^0(q) - Y(q)A(q) \\ T(q) &= X(q)T^0(q) \end{aligned} \quad (18)$$

the system output follows:

$$y(t) = \frac{X(q)A_0(q)B_m(q)}{X(q)A_0(q)A_m(q)} u_{\mathrm{c}}(t) + \frac{B(q)R'(q)}{X(q)A_0(q)A_m(q)} e(t). \quad (19)$$

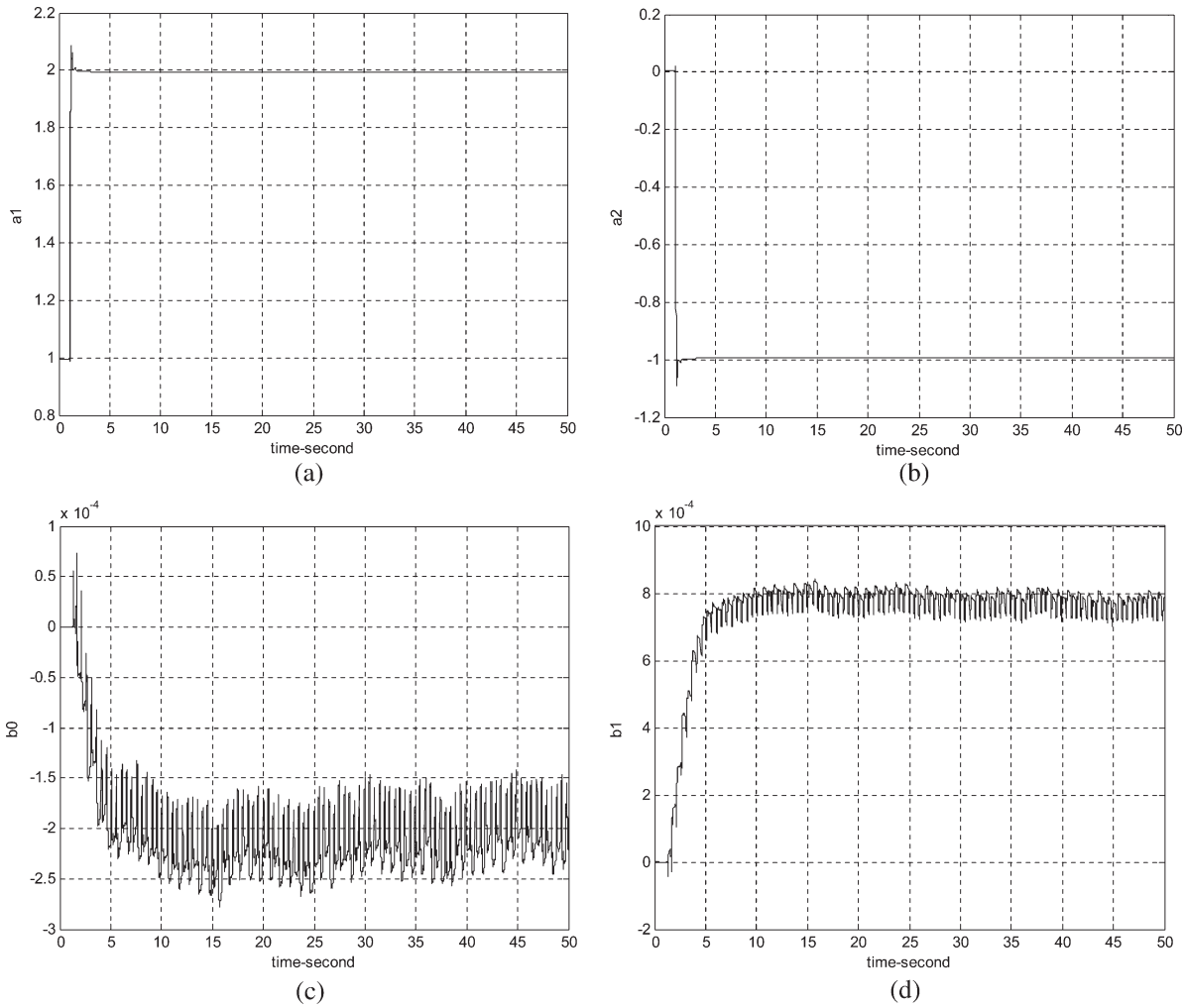

Fig. 10. Estimating the parameters of the LSRM: (a) a1, (b) a2, (c) b0, and (d) b1.

From (19), it can be seen that the system output can track the input command in a desired response and is insensitive to the load disturbances. The closed-loop pole equation is changed to $X(q)A_0(q)A_m(q)$. For keeping the stability of the system, $A_0(q)$ and $X(q)$ should be chosen as stable polynomials. In this paper, the plant is a second-order system described as (6), and the regulator is designed by the pole placement algorithm without zero cancellation. Choosing stable polynomials $A_0(q)$ and $X(q)$, the parameters of the regulator can be obtained by solving the (15), (18), and (19), then the control law can be calculated from (12).

IV. Simulation Results

In this section, we illustrate the performance of the proposed STR by simulations. The simulations are achieved with the MATLAB software package. Also, the parameter values of the LSRM system employed in the simulations are listed in the Table I. In some industrial applications, the performance of overshoot free is required. In the simulations, the poles of the reference model are chosen as $a_{1m} = -1.912$ and $a_{2m} = 0.9139$, the observer polynomial is chosen as $q + 0.5$, $X(q^{-1})$ is chosen as $q + 0.8$ and the sampling time is set to 0.001 s. This parameter selection can make the LSRM system overshoot free. Fig. 5 shows the response waveforms and control signals for the STR and a conventional proportional-derivative (PD) control. The PD controller is set in the initial condition with 100% system gain. From the figure, both of the two controllers have good performance. Figs. 6–8 demonstrate the response waveforms for the two controllers in different parameters of the LSRM. In Fig. 6, the mass of the moving platform is increased to twice as in Fig. 5; in Fig. 7, the mass of the moving platform is increased to twice as in Fig. 5 and the system gain is reduced to the 50%; in Fig. 8, besides the mass and system gain changed as in Fig. 7, there is an external load disturbance applied on the LSRM model. It can be seen that the response waveforms for the PD controller changed with the parameters of the LSRM while the STR can keep its response waveform invariable and overshoot free. Hence, the STR is very robust to the change of the system parameters.

V. Experimental Implementation Results

The experimental setup is shown in Fig. 9. The host PC is a Pentium 4 computer that is used to download the target code into a dSPACE DS1104 DSP motion controller card. The

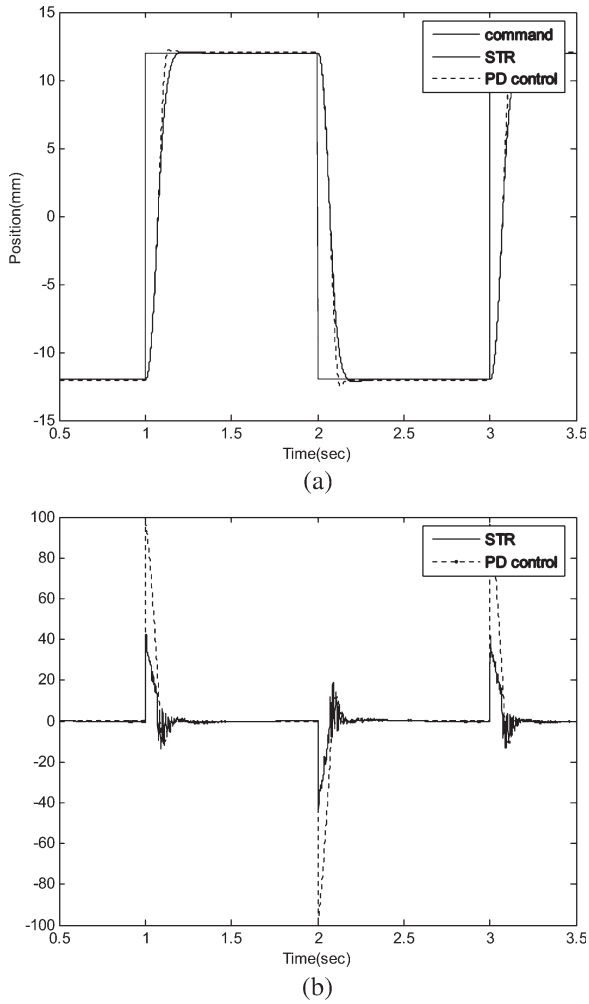

Fig. 11. (a) Position tracking waveforms and (b) the controller output waveforms with 100% system gain.

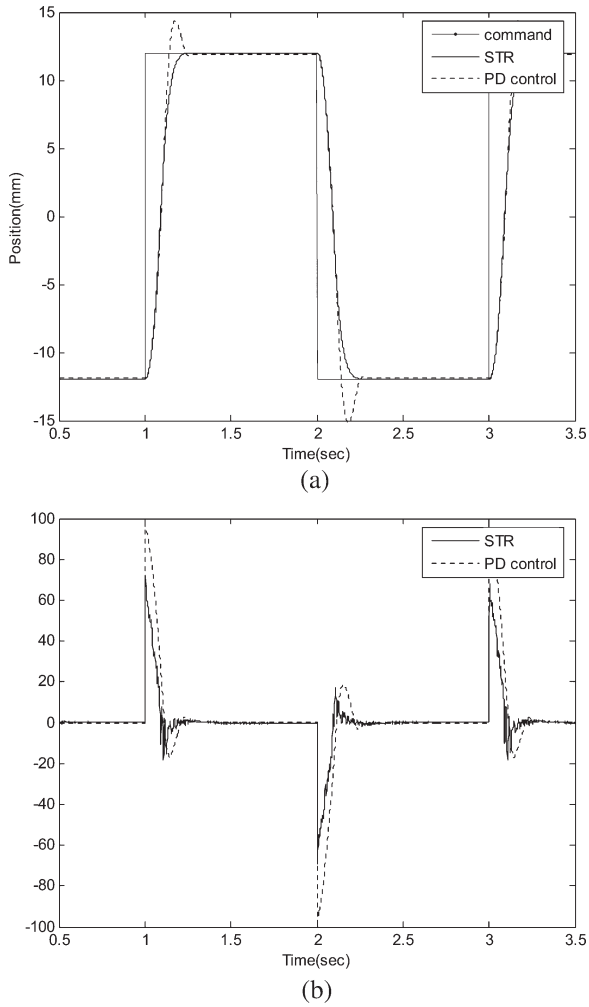

Fig. 12. (a) Position tracking waveforms and (b) the controller output waveforms with the 200% mass increase on the moving platform.

control algorithm is developed under the MATLAB/SIMULINK environment. All control functions are implemented by the DS1104 card, which is plugged into a PCI bus of the host PC. For the current tracking amplifier, the driver consists of three asymmetric bridge insulated-gate-bipolar-transistor inverters with 90 VDC voltage supplier. A linear optical encoder with 0.5-μm-resolution is mounted on the mover of the LSRM system and provides position feedback information. In the experiment, the control signal is the sum of the weighted PD control signal and self-tuning regulating signal. At the beginning, the LSRM is operated by the PD controller. Then, the control signal is switched on continuously a few seconds later. Finally, the LSRM is fully operated by the STR. Because of lack of the prior knowledge about the plant, a displacement impact for the LSRM would be resulted if the self-tuning regulating is fully switched on at the beginning of the operation. However, the weighted control method can avoid the impact of motor at the beginning of the operation.

In the experiment, the LSRM system is considered as a second-order system (6) with a sampling time of 0.001 s. Equation (7) is used as the parameter estimation model. Fig. 10 shows the parameters estimating of the LSRM system. The figures show that the parameters converge to their stable values very quickly. Parameters a_1 and a_2 can converge to their stable values within 2 s, while parameters b_0 and b_1 can converge to their stable values in about 8 s.

Fig. 11 shows the position tracking waveforms and its corresponding control signal waveforms in the control of the proposed STR and a conventional PD controller with the 100% system gain. Since the parameters of the PD controller cannot change, they are set under the condition of 100% system gain. It can be seen that both of two controllers can obtain good dynamic performance and accurate position tracking. Figs. 12–14 show the corresponding experimental results with the different system parameters. In Fig. 12, the mass of the moving platform is increased to twice of in Fig. 11; in Fig. 13, the mass of the moving platform is increased to twice and the system gain is reduced to the 50%; in Fig. 14, besides the mass of the moving platform and system gain changed as in Fig. 13, there is an external load disturbance acted on the LSRM. The figures confirm that the response waveforms of the STR remain the same under different parameter changes and operating conditions, while the PD control has different

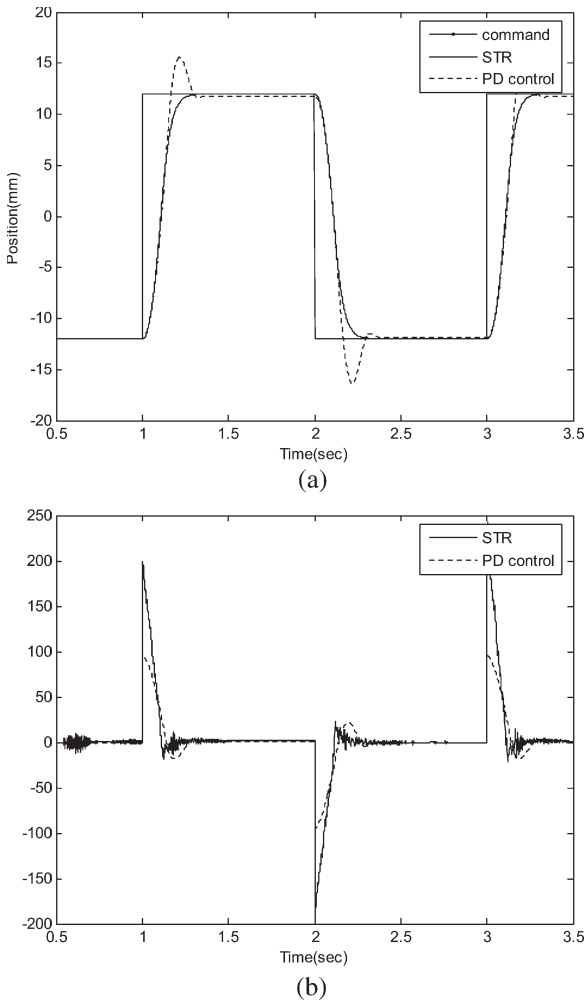

Fig. 13. (a) Position tracking waveforms and (b) the controller output waveforms with 50% system gain and 200% mass increase on the moving platform.

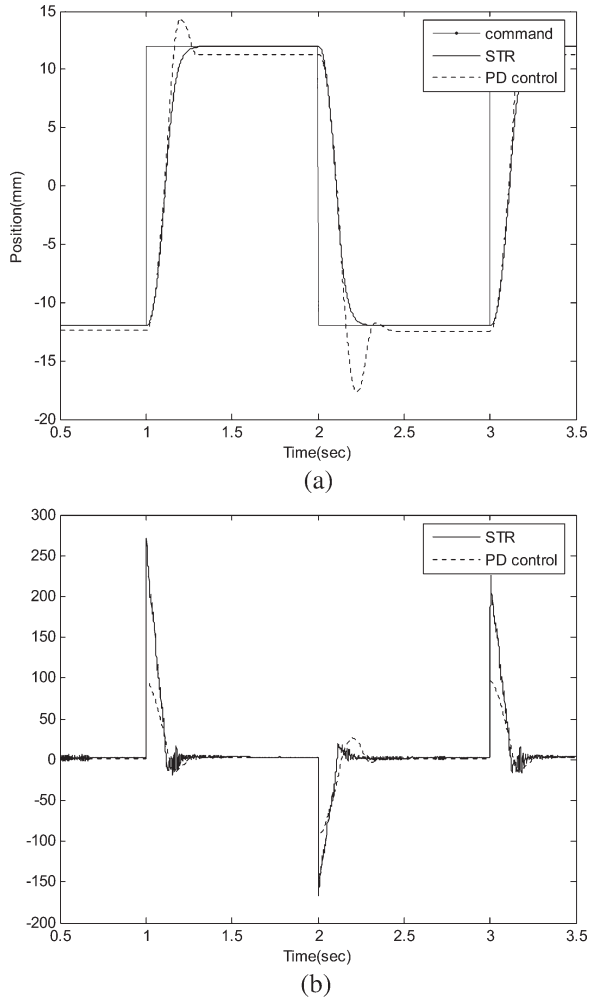

Fig. 14. (a) Trajectory response and (b) control signal of the LSRM system with 50% system gain, 200% mass increase on the moving platform, and an external load disturbance.

dynamic responses. The experimental results are very similar to the simulation results. The overshoot of the output waveform for the PD controller increase substantially when the parameters of the LSRM system are changed. There is no overshoot for the STR under all operating conditions. The experiment data confirmed that the proposed STR is more robust and has a higher performance than the conventional PD controller.

VI. Conclusion

This paper proposes a STR based for the high-precision control of the LSRM. First, the motor winding excitation scheme and the model of the LSRM with current control are introduced. Then, the LSRM system is represented by a single-input single-output discrete model. After this, parameter estimation method and a STR based on the pole placement algorithm are developed for the position tracking of the LSRM. Both the simulation and experimental results demonstrate that the parameters can converge quickly. Also, under the STR, the position tracking of the LSRM has almost no influence when the system parameters are changed. The position output remains overshoot free irrespective of the parameter changes. These results confirm that the method is effective and robust in the position tracking of the LSRM.

References

[1] K. J. Astrom and B. Wittenmark, *Adaptive Control*. Reading, MA: Addison-Wesley, 1995.

[2] B. S. Lee, H. K. Bae, P. Vijayraghavan, and R. Krishnan, "Design of a linear switched reluctance machines," *IEEE Trans. Ind. Appl.*, vol. 36, no. 6, pp. 1571–1580, Nov./Dec. 2000.

[3] W. C. Gan and N. C. Cheung, "Design of a linear switched reluctance motor for high precision applications," in *Proc. IEEE IEMDC*, 2001, pp. 701–704.

[4] W. C. Gan and N. C. Cheung, "A low-cost linear switched reluctance motor with integrated position sensor for general-purpose three-phase motor controller," in *Proc. IECON*, Nov. 29/Dec. 2, 2001, vol. 1, pp. 468–473.

[5] U. S. Deshpande, J. J. Cathey, and E. Richter, "A high force density linear switched reluctance machine," in *Proc. Ind. Appl. Soc. Annu. Meeting*, Oct. 2–8, 1993, vol. 31, pp. 251–257.

[6] U. S. Deshpande, J. J. Cathey, and E. Richter, "High-force density linear switched reluctance machine," *IEEE Trans. Ind. Appl.*, vol. 31, no. 2, pp. 345–352, Mar./Apr. 1995.

[7] H. K. Bae, B. S. Lee, P. Vijayraghavan, and R. Krishnan, "A linear switched reluctance motor: Converter and control," *IEEE Trans. Ind. Appl.*, vol. 36, no. 5, pp. 1351–1359, Sep./Oct. 2000.

[8] J. L. Dorningos, D. A. Andrade, M. A. A. Freitas, and H. De Paula, "A new drive strategy for a linear switched reluctance motor," in *Proc. IEMDC*, 2003, vol. 3, pp. 1714–1719.
[9] J. F. Pan, S. C. Kwok, N. C. Cheung, and J. M. Yang, "Auto disturbance rejection speed control of linear switched reluctance motor," in *Proc. Ind. Appl. Conf. (IAS)*, Oct. 2–6, 2005, vol. 4, pp. 2491–2497.
[10] W. C. Gan, N. C. Cheung, and L. Qiu, "Position control of linear switched reluctance motors for high precision applications," *IEEE Trans. Ind. Appl.*, vol. 39, no. 5, pp. 1350–1362, Sep./Oct. 2003.
[11] F. Khorrami, P. Krishnamurthy, and H. Melkote, *Modeling and Adaptive Nonlinear Control of Electric Motors*. Berlin, Germany: Springer-Verlag, 2003.
[12] W. C. Gan and N. C. Cheung, "Development and control of a low-cost linear variable reluctance motor for precision manufacturing automation," *IEEE/ASME Trans. Mechatronics*, vol. 8, no. 3, pp. 326–333, Sep. 2003.
[13] S. S. Wilson and C. L. Carnal, "System identification with disturbances," in *Proc. 26th Southeastern Symp. Syst. Theory*, Mar. 1994, pp. 502–506.

Shi Wei Zhao (S'07) received the B.Sc. degree from Central South University, Changsha, China, in 2000, and the M.Sc. degree from South China University of Technology, Guangzhou, China, in 2003. He is currently working toward the Ph.D. degree at the Department of Electrical Engineering, Hong Kong Polytechnic University, Kowloon, Hong Kong.

His main research interests are motion control and machine drives.

Norbert C. Cheung (S'85–M'91–SM'05) received the B.Sc. degree from the University of London, London, U.K., in 1981, the M.Sc. degree from the University of Hong Kong, in 1987, and the Ph.D. degree from the University of New South Wales, Kensington, NSW, Australia, in 1995.

He is currently working in the Department of Electrical Engineering, Hong Kong Polytechnic University, Kowloon, Hong Kong. His research interests are motion control, actuators design, and power electronic drives.

Wai-Chuen Gan (S'94–M'02–SM'07) received the B.Eng. degree (with first-class honors and the academic achievement award) in electronic engineering, and the M.Phil. and Ph.D. degrees in electrical and electronic engineering from Hong Kong University of Science and Technology, Clear Water Bay, Hong Kong, in 1995, 1997, and 2001, respectively.

From 1997 to 1999, he was a Motion Control Application Engineer at ASM Assembly Automaton, Ltd., Hong Kong. He rejoined the same company in 2002 and is responsible for the development of the digital motor drivers. His current research interests include robust control of ac machines, power electronics, design and control of linear switched reluctance motors, and control of steeping motors via interconnection and damping assignment.

Jin Ming Yang received the B.Sc. degree from the University of Beijing Aeronautics, Beijing, China, in 1987, the M.Sc. degree from Zhejiang University, Hangzhou, Zhejiang, China, in 1990, and the Ph.D. degree from South China University of Technology, Guangzhou, China, in 2000.

He is currently an Associate Professor at the South China University of Technology. His research interests are machine drives and nonlinear control.

Jian Fei Pan (S'04) was born in Harbin, China, in 1978. He received the B.Sc. degree in electrical engineering from ChangChun University of Science and Technology, ChangChun, China, in 2001. He is currently working toward the Ph.D. degree at the Department of Electrical Engineering, Hong Kong Polytechnic University, Kowloon, Hong Kong.

His main research interest is in the control of switched reluctance devices.